SLAC-PUB-95-6971
August 4, 1995
(N)

Measurement of the τ Charged Weak Couplings with SLC Polarized Beams[1]

The SLD Collaboration*

Stanford Linear Accelerator Center

Stanford University, Stanford, CA 94309

Abstract

We present a measurement of the tau neutrino helicity, h_{ν_τ}, and the Michel parameters, ξ and δ, by analyzing the τ decays $\tau\rightarrow\pi(K)\nu_\tau$, $\tau\rightarrow e\bar{\nu}_e\nu_\tau$ and $\tau\rightarrow\mu\bar{\nu}_\mu\nu_\tau$ in $e^+e^- \rightarrow Z^0 \rightarrow \tau^+\tau^-$. The analysis uses the 1993-1995 SLD data sample of 4552 τ-pair events produced with highly polarized electrons. We obtain preliminary results of $h_{\nu_\tau} = -0.89 \pm 0.21 \pm 0.07$, $\xi = 1.17 \pm 0.35 \pm 0.21$ and $\xi\delta = 0.49 \pm 0.24 \pm 0.13$.

Submitted to the 1995 International Symposium on Lepton and Photon Interactions at High Energies, Beijing, China

[1]This work was supported by Department of Energy contracts: DE-FG02-91ER40676 (BU), DE-FG03-92ER40701 (CIT), DE-FG03-91ER40618 (UCSB), DE-FG03-92ER40689 (UCSC), DE-FG03-93ER40788 (CSU), DE-FG02-91ER40672 (Colorado), DE-FG02-91ER40677 (Illinois), DE-AC03-76SF00098 (LBL), DE-FG02-92ER40715 (Massachusetts), DE-AC02-76ER03069 (MIT), DE-FG06-85ER40224 (Oregon), DE-AC03-76SF00515 (SLAC), DE-FG05-91ER40627 (Tennessee), DE-AC02-76ER00881 (Wisconsin), DE-FG02-92ER40704 (Yale); National Science Foundation grants: PHY-91-13428 (UCSC), PHY-89-21320 (Columbia), PHY-92-04239 (Cincinnati), PHY-88-17930 (Rutgers), PHY-88-19316 (Vanderbilt), PHY-92-03212 (Washington); the UK Particle Physics and Astronomy Research Council (Brunel and RAL); the Istituto Nazionale di Fisica Nucleare of Italy (Bologna, Ferrara, Frascati, Pisa, Padova, Perugia); and the Japan-US Cooperative Research Project on High Energy Physics (Nagoya, Tohoku).

The SLD Collaboration*

K. Abe,[29] I. Abt,[14] C.J. Ahn,[26] T. Akagi,[27] N.J. Allen,[4] W.W. Ash,[27]† D. Aston,[27] K.G. Baird,[25] C. Baltay,[33] H.R. Band,[32] M.B. Barakat,[33] G. Baranko,[10] O. Bardon,[16] T. Barklow,[27] A.O. Bazarko,[11] R. Ben-David,[33] A.C. Benvenuti,[2] T. Bienz,[27] G.M. Bilei,[22] D. Bisello,[21] G. Blaylock,[7] J.R. Bogart,[27] T. Bolton,[11] G.R. Bower,[27] J.E. Brau,[20] M. Breidenbach,[27] W.M. Bugg,[28] D. Burke,[27] T.H. Burnett,[31] P.N. Burrows,[16] W. Busza,[16] A. Calcaterra,[13] D.O. Caldwell,[6] D. Calloway,[27] B. Camanzi,[12] M. Carpinelli,[23] R. Cassell,[27] R. Castaldi,[23][a] A. Castro,[21] M. Cavalli-Sforza,[7] E. Church,[31] H.O. Cohn,[28] J.A. Coller,[3] V. Cook,[31] R. Cotton,[4] R.F. Cowan,[16] D.G. Coyne,[7] A. D'Oliveira,[8] C.J.S. Damerell,[24] M. Daoudi,[27] R. De Sangro,[13] P. De Simone,[13] R. Dell'Orso,[23] M. Dima,[9] P.Y.C. Du,[28] R. Dubois,[27] B.I. Eisenstein,[14] R. Elia,[27] E. Etzion,[4] D. Falciai,[22] M.J. Fero,[16] R. Frey,[20] K. Furuno,[20] T. Gillman,[24] G. Gladding,[14] S. Gonzalez,[16] G.D. Hallewell,[27] E.L. Hart,[28] Y. Hasegawa,[29] S. Hedges,[4] S.S. Hertzbach,[17] M.D. Hildreth,[27] J. Huber,[20] M.E. Huffer,[27] E.W. Hughes,[27] H. Hwang,[20] Y. Iwasaki,[29] D.J. Jackson,[24] P. Jacques,[25] J. Jaros,[27] A.S. Johnson,[3] J.R. Johnson,[32] R.A. Johnson,[8] T. Junk,[27] R. Kajikawa,[19] M. Kalelkar,[25] H. J. Kang,[26] I. Karliner,[14] H. Kawahara,[27] H.W. Kendall,[16] Y. Kim,[26] M.E. King,[27] R. King,[27] R.R. Kofler,[17] N.M. Krishna,[10] R.S. Kroeger,[18] J.F. Labs,[27] M. Langston,[20] A. Lath,[16] J.A. Lauber,[10] D.W.G. Leith,[27] M.X. Liu,[33] X. Liu,[7] M. Loreti,[21] A. Lu,[6] H.L. Lynch,[27] J. Ma,[31] G. Mancinelli,[22] S. Manly,[33] G. Mantovani,[22] T.W. Markiewicz,[27] T. Maruyama,[27] R. Massetti,[22] H. Masuda,[27] E. Mazzucato,[12] A.K. McKemey,[4] B.T. Meadows,[8] R. Messner,[27] P.M. Mockett,[31] K.C. Moffeit,[27] B. Mours,[27] G. Müller,[27] D. Muller,[27] T. Nagamine,[27] U. Nauenberg,[10] H. Neal,[27] M. Nussbaum,[8] Y. Ohnishi,[19] L.S. Osborne,[16] R.S. Panvini,[30] H. Park,[20] T.J. Pavel,[27] I. Peruzzi,[13][b] M. Piccolo,[13] L. Piemontese,[12] E. Pieroni,[23] K.T. Pitts,[20] R.J. Plano,[25] R. Prepost,[32] C.Y. Prescott,[27] G.D. Punkar,[27] J. Quigley,[16] B.N. Ratcliff,[27] T.W. Reeves,[30] J. Reidy,[18] P.E. Rensing,[27] L.S. Rochester,[27] J.E. Rothberg,[31] P.C. Rowson,[11] J.J. Russell,[27] O.H. Saxton,[27] S.F. Schaffner,[27] T. Schalk,[7] R.H. Schindler,[27] U. Schneekloth,[16] B.A. Schumm,[15] A. Seiden,[7] S. Sen,[33] V.V. Serbo,[32] M.H. Shaevitz,[11] J.T. Shank,[3] G. Shapiro,[15] S.L. Shapiro,[27] D.J. Sherden,[27] K.D. Shmakov,[28] C. Simopoulos,[27] N.B. Sinev,[20] S.R. Smith,[27] J.A. Snyder,[33] P. Stamer,[25] H. Steiner,[15] R. Steiner,[1] M.G. Strauss,[17] D. Su,[27] F. Suekane,[29] A. Sugiyama,[19] S. Suzuki,[19] M. Swartz,[27] A. Szumilo,[31] T. Takahashi,[27] F.E. Taylor,[16] E. Torrence,[16] J.D. Turk,[33] T. Usher,[27] J. Va'vra,[27] C. Vannini,[23] E. Vella,[27] J.P. Venuti,[30] R. Verdier,[16] P.G. Verdini,[23] S.R. Wagner,[27] A.P. Waite,[27] S.J. Watts,[4] A.W. Weidemann,[28] E.R. Weiss,[31] J.S. Whitaker,[3] S.L. White,[28] F.J. Wickens,[24] D.A. Williams,[7] D.C. Williams,[16] S.H. Williams,[27] S. Willocq,[33] R.J. Wilson,[9] W.J. Wisniewski,[5] M. Woods,[27] G.B. Word,[25] J. Wyss,[21] R.K. Yamamoto,[16] J.M. Yamartino,[16] X. Yang,[20] S.J. Yellin,[6] C.C. Young,[27] H. Yuta,[29] G. Zapalac,[32] R.W. Zdarko,[27] C. Zeitlin,[20] Z. Zhang,[16] and J. Zhou,[20]

[1]*Adelphi University, Garden City, New York 11530*
[2]*INFN Sezione di Bologna, I-40126 Bologna, Italy*
[3]*Boston University, Boston, Massachusetts 02215*
[4]*Brunel University, Uxbridge, Middlesex UB8 3PH, United Kingdom*
[5]*California Institute of Technology, Pasadena, California 91125*
[6]*University of California at Santa Barbara, Santa Barbara, California 93106*
[7]*University of California at Santa Cruz, Santa Cruz, California 95064*
[8]*University of Cincinnati, Cincinnati, Ohio 45221*
[9]*Colorado State University, Fort Collins, Colorado 80523*
[10]*University of Colorado, Boulder, Colorado 80309*
[11]*Columbia University, New York, New York 10027*
[12]*INFN Sezione di Ferrara and Università di Ferrara, I-44100 Ferrara, Italy*
[13]*INFN Lab. Nazionali di Frascati, I-00044 Frascati, Italy*
[14]*University of Illinois, Urbana, Illinois 61801*
[15]*Lawrence Berkeley Laboratory, University of California, Berkeley, California 94720*
[16]*Massachusetts Institute of Technology, Cambridge, Massachusetts 02139*
[17]*University of Massachusetts, Amherst, Massachusetts 01003*
[18]*University of Mississippi, University, Mississippi 38677*
[19]*Nagoya University, Chikusa-ku, Nagoya 464 Japan*
[20]*University of Oregon, Eugene, Oregon 97403*
[21]*INFN Sezione di Padova and Università di Padova, I-35100 Padova, Italy*
[22]*INFN Sezione di Perugia and Università di Perugia, I-06100 Perugia, Italy*
[23]*INFN Sezione di Pisa and Università di Pisa, I-56100 Pisa, Italy*
[25]*Rutgers University, Piscataway, New Jersey 08855*
[24]*Rutherford Appleton Laboratory, Chilton, Didcot, Oxon OX11 0QX United Kingdom*
[26]*Sogang University, Seoul, Korea*
[27]*Stanford Linear Accelerator Center, Stanford University, Stanford, California 94309*
[28]*University of Tennessee, Knoxville, Tennessee 37996*
[29]*Tohoku University, Sendai 980 Japan*
[30]*Vanderbilt University, Nashville, Tennessee 37235*
[31]*University of Washington, Seattle, Washington 98195*
[32]*University of Wisconsin, Madison, Wisconsin 53706*
[33]*Yale University, New Haven, Connecticut 06511*
†*Deceased*
[a]*Also at the Università di Genova*
[b]*Also at the Università di Perugia*

1 Introduction

The weak couplings of the tau may be studied by investigating the energy spectra of various tau decay products. These spectra are determined by the spin polarization of the taus and the nature of the decay [1].

At the Z^0 , taus are produced with spin polarization due to the inherent parity violation of the Z^0 couplings. At the SLC, this is enhanced due to the electron beam polarization. We can write the production cross sections for left and right handed taus as follows:

$$\begin{aligned}
\frac{1}{\sigma_{tot}}\frac{d\sigma_L}{d\cos\theta} &= \tfrac{3}{16}(1+\mathrm{A}_\tau)[(1-\mathrm{A}_e P_e)(1+\cos^2\theta)+2(\mathrm{A}_e-P_e)\cos\theta], \\
\frac{1}{\sigma_{tot}}\frac{d\sigma_R}{d\cos\theta} &= \tfrac{3}{16}(1-\mathrm{A}_\tau)[(1-\mathrm{A}_e P_e)(1+\cos^2\theta)-2(\mathrm{A}_e-P_e)\cos\theta],
\end{aligned} \tag{1}$$

where θ is the polar angle of the τ^- (τ^+) with respect to the incident electron (positron) direction, P_e is the electron beam polarization, and A_e and A_τ are the electron and tau parity-violation asymmetry parameters defined as:

$$\mathrm{A}_\ell = \frac{2\hat{g}_v^\ell/\hat{g}_a^\ell}{1+(\hat{g}_v^\ell/\hat{g}_a^\ell)^2}, \tag{2}$$

where $\hat{g}_v^\ell/\hat{g}_a^\ell$ is the ratio between the effective Z^0 vector and axial-vector couplings to the leptons.

This results in the following expression for the tau polarization as a function of angle and beam polarization:

$$P_\tau(\cos\theta, P_e) = \frac{\frac{d\sigma_R}{d\cos\theta}-\frac{d\sigma_L}{d\cos\theta}}{\frac{d\sigma_R}{d\cos\theta}+\frac{d\sigma_L}{d\cos\theta}} = -\frac{\mathrm{A}_\tau + 2\frac{\mathrm{A}_e-P_e}{1-\mathrm{A}_eP_e}\frac{\cos\theta}{1+\cos^2\theta}}{1+2\mathrm{A}_\tau\frac{\mathrm{A}_e-P_e}{1-\mathrm{A}_eP_e}\frac{\cos\theta}{1+\cos^2\theta}}. \tag{3}$$

Due to the large beam polarization at SLC, tau polarizations are much higher than at LEP, especially at high $|\cos\theta|$ (see Fig. 1). Also, the polarization of the tau is largely determined by the beam polarization and the production angle, and is relatively unaffected by the Z^0 parity violation.

In this paper, we study the energy spectra of taus decaying to pions, electrons and muons. Taus produced at the Z^0 are highly boosted, and as a result, angular information about the decays is lost due to the collimation of the decay. In the case of a two body decay, such as $\tau\rightarrow\pi(\mathrm{K})\nu_\tau$, the decay spectrum at rest is mono-energetic, so the boosted energy spectrum merely reflects the angle of the pion in the rest frame. In the case of a three body decay, such as $\tau\rightarrow\mu\bar{\nu}_\mu\nu_\tau$ or $\tau\rightarrow e\bar{\nu}_e\nu_\tau$, the boosted energy spectrum is a combination of both the rest frame angular distribution and energy spectra. In all of these cases, we can parameterize the decay spectrum in two parts, a constant part that is unaffected by the

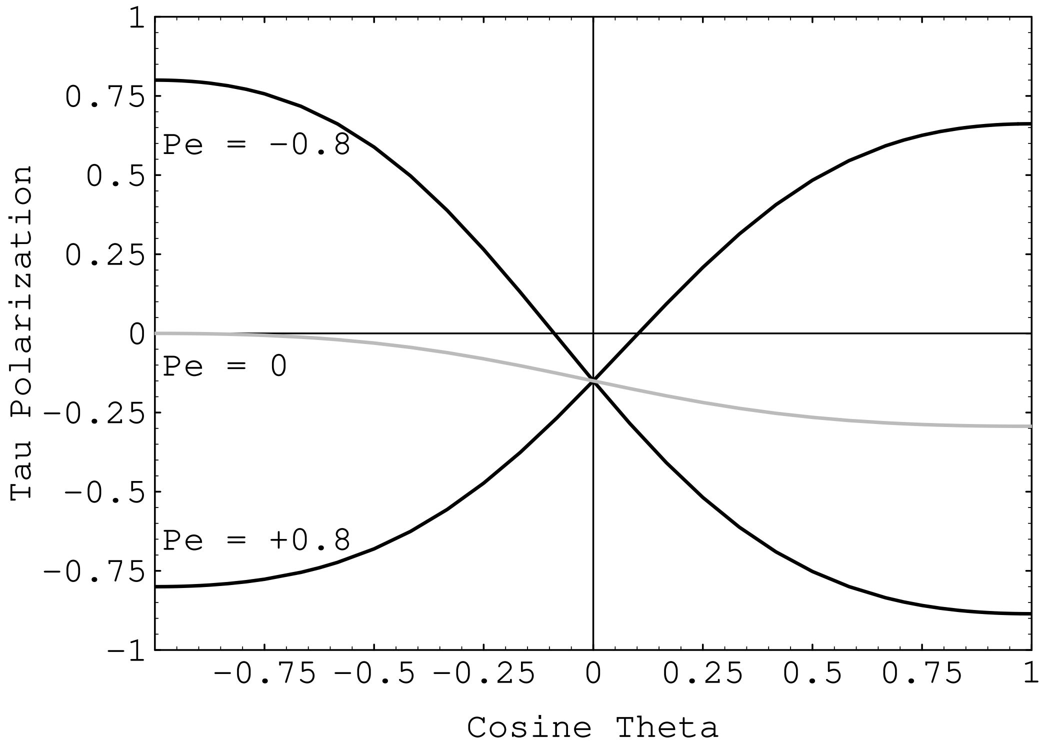

Figure 1: Tau polarization vs production angle with and without beam polarization.

handedness of the tau, and a polarization dependent part that changes sign depending on the handedness of the tau:

$$\begin{aligned}\frac{1}{\Gamma}\frac{d\Gamma_L}{dx} &= f(x) + g(x),\\ \frac{1}{\Gamma}\frac{d\Gamma_R}{dx} &= f(x) - g(x).\end{aligned} \tag{4}$$

In the case of the pion (kaon), we can describe this with one parameter, h_{ν_τ}, which characterizes the polarization dependent term. We get the following decay spectrum for $\tau \rightarrow \pi(\mathrm{K})\nu_\tau$:

$$\begin{aligned} f(x) &= 1,\\ g(x) &= \mathrm{h}_{\nu_\tau}\frac{2x - 1 - m_h^2/m_\tau^2}{1 - m_h^2/m_\tau^2}, \end{aligned} \tag{5}$$

where m_τ^2 and m_h^2 are the masses of the τ and the decayed hadron respectively, and x is the hadron's energy scaled by the τ energy ($x = \frac{E_\pi}{E_T}$).

In the case of the leptons, neglecting mass differences, we can describe the energy spectrum with the three Michel parameters[1] ρ, ξ and δ. Here the parameter ρ describes the

[1] These parameters were originally conceived to describe muon decay [2]. They describe the energy and

non-polarization-dependent term, and ξ and δ describe the polarization dependent terms. We get the following spectrum for $\tau \rightarrow \ell \bar{\nu}_\ell \nu_\tau$:

$$\begin{aligned} f(x) &= f_1 + \rho \cdot f_2, \\ g(x) &= \xi(g_1 + \delta \cdot g_2), \end{aligned} \tag{6}$$

where

$$\begin{aligned} f_1 &= 2 - 6x^2 + 4x^3, \\ f_2 &= \frac{4}{9}(-1 + 9x^2 - 8x^3), \\ g_1 &= -\frac{2}{3} + 4x - 6x^2 + \frac{8}{3}x^3, \quad and \\ g_2 &= \frac{4}{9}(1 - 12x + 27x^2 - 16x^3)]. \end{aligned} \tag{7}$$

Here $x = \frac{E_\ell}{E_\mathcal{T}}$.

These decay spectra are combined with the production cross sections to get theoretical decay distributions:

$$\frac{1}{\sigma}\frac{d^2\sigma(x, \cos\theta, P_e)}{dx d\cos\theta} = \frac{d\sigma_L}{d\cos\theta}\frac{1}{\Gamma}\frac{d\Gamma_L}{dx} + \frac{d\sigma_R}{d\cos\theta}\frac{1}{\Gamma}\frac{d\Gamma_R}{dx}. \tag{8}$$

These can be rewritten as:

$$\frac{1}{\sigma}\frac{d^2\sigma(x, \cos\theta, P_e)}{dx d\cos\theta} = f(x) - P_\mathcal{T}(\cos\theta, P_e) \cdot g(x), \tag{9}$$

which clearly illustrates the importance of high tau polarization for measuring the polarization dependent terms. For τ^+ decays, the sign of the polarization dependent term is reversed due the opposite helicity of the anti-neutrino. However, since at the Z^0 taus are produced in pairs with opposite helicities, if the τ^- direction is used as the lab frame variable the τ^- and τ^+ decay spectra are identical.

2 Apparatus

The results reported here are based on a sample of 4522 tau-pair candidates collected by the SLC Large Detector (SLD) during the period 1993-1995. The 1993 run accumulated an integrated luminosity of 1.78 pb^{-1} with an average electron beam polarization of 63%, and the 1994-1995 run accumulated 3.66 pb^{-1} with an average polarization of 77%. A general description of the SLD can be found elsewhere [4]. Charged particle tracking and momentum analysis are provided by the Central Drift Chamber (CDC) [5] and the CCD-based vertex detector [6] in a uniform axial magnetic field of 0.6 T. Particle energies are measured in the

the angular spectrum of the resultant electron with respect to the initial muon spin direction. Lepton universality implies that the tau Michel parameters should be identical to the well measured muon Michel parameters [3].

Liquid Argon Calorimeter (LAC) [7], which is segmented into projective towers with separate electromagnetic and hadronic sections. The measured energy and the shape of the energy flow are used to distinguish between different particles. Additional particle identification is provided by a Čerenkov Ring-Imaging Detector (CRID) [8], and muons are identified and tracked in the Warm Iron Calorimeter (WIC) [9].

The SLD event trigger requires any of several combinations of tracking and energy-flow information from the detector elements. A subset of these have a relatively high efficiency for tau-pair events, in particular a requirement of at least two back-to-back tracks, or a single track plus a minimum energy deposition in the calorimeter.

3 Event Selection

The selection of tau-pair candidates at SLD (as given in Ref. [10]) is based on the multiplicity, momentum and direction of tracks in the central drift chamber, and on properties of electromagnetic showers in the calorimeter. Candidates are required to have at least two but fewer than seven tracks. Each event is divided into hemispheres by the plane normal to the track with the highest momentum. Tracks in each hemisphere must fall within 15° cone of the net momentum vector in the hemisphere, and the cone invariant mass in each hemisphere is required to be less than 2.3 GeV/c^2. Furthermore, the cone axes in the two hemispheres must be back-to-back within 20°. These criteria discriminate strongly against background from multi-hadron final states. The polar angle Θ_{miss} of the missing momentum in each event is required to satisfy $|\cos\Theta_{miss}| < 0.88$ to discriminate against two-photon interactions and Bhabha events. Two-prong events are required to have a minimum acolinearity of 10 mrad. The scalar sum of the momenta of the two stiffest tracks in any event must be less than 65 GeV/c. These cuts primarily reject Bhabha events and muon-pair final states.

The total visible energy in an event is required to be at least 12% of the center-of-mass energy (E_{CM}) to reject two-photon interactions. To discriminate against Bhabha events, the total energy deposited in the electromagnetic section of the calorimeter is required to be less than 0.45 E_{CM}, and the most energetic EM cluster must be less than 0.33 E_{CM}. In addition, the total calorimeter energy not included in a cone is required to be less than 5 GeV, and there must be fewer than six energy clusters not included in the cones.

These criteria resulted in a sample of 4522 tau-pair candidates selected from the 1993-1995 data. The event selection efficiency and background contamination were estimated using Monte Carlo. The production of tau-pair events at the Z^0 resonance was simulated using the KORALZ [11] Monte Carlo generator. The same program was used to generate muon-pair events, while wide-angle Bhabha scattering, two-photon interactions, and $Z^0 \to$ *hadrons* final states were produced using the generators described in Refs. [12], [13], and [14], respectively. All these Monte Carlo data samples were subjected to the SLD detector simulation based on the GEANT [15] program and to the above event selection. The SLD trigger was also simulated in the Monte Carlo.

Identification of Tau Decays

Selected tau events are divided into hemispheres by the plane normal to the event thrust axis, and the hemispheres are treated independently. Any pairs of oppositely charged tracks which are consistent with originating from a photon conversion are removed, and hemispheres are then required to have only a single track.

For the selection of tau decays to single pions (or kaons), tracks are required to have no unassociated electromagnetic (EM) LAC energy clusters within 10^o of the thrust axis. This requirement is powerful for rejecting backgrounds from decays into ρ or a_1. Electrons and muons are rejected by a series of hybrid cuts applied with increasing strength, making use of the electromagnetic and muon calorimeter information. The information used consists of E/p, hadronic energy, cluster shape, and energy deposited in the WIC. For the tracks that are left, the associated EM cluster must have fewer than 16 hit towers and the track momentum must be greater than 3 GeV/c. A further requirement of $E_{EM}/p < 0.3$ is made, and a quasi-invariant mass is calculated assuming that the associated cluster energy originated from photons and that the track is a pion. This quantity is required to be less than 0.3 GeV/c^2.

Finally, due to the barrel WIC angular coverage, the remaining tracks are divided into two regions, namely $|cos\theta| < 0.62$ and $0.62 < |cos\theta| < 0.74$. The total energy in the LAC divided by the track momentum is required to be greater than 0.1 in the former and 0.3 in the latter case. These criteria discriminate effectively against muons.

This selection provides a sample of 411 tracks identified as $\tau \rightarrow \pi(\mathrm{K})\nu_\tau$ from the 1993-1995 data, with an efficiency of approximately 48% and a purity of 84%. The selection efficiency and background fraction for these decays are plotted in Fig. 2(a) and 2(b) as a function of the scaled energy of the track.

For tau decays to muons, the sample is divided into the same polar angle regions as above. In the region of $|\cos\theta| < 0.62$, the WIC is used to identify muons by associating WIC hits with CDC tracks. In the $0.62 < |\cos\theta| < 0.74$ region, shower information from the LAC is used instead. We require that E/p be less than 0.3, that the total number of electromagnetic LAC towers hit in the associated cluster be less than 4, and that there be no unassociated neutral clusters within 10^o of the track. In addition, the quasi-invariant mass (calculated as above) is required to be less than 180 MeV/c^2. This results in a sample of 1137 tracks identified as muons, with an estimated selection efficiency of 92% within the acceptance, and an estimated purity of 94%. Fig. 2(c) and 2(d) show the selection efficiency and background fraction for these tracks.

Criteria for selection of tau decays to electrons are consistent over the full range $|\cos\theta| < 0.74$. The LAC shower shape must be consistent with that of an electron, or any valid CRID data must strongly favor the electron hypothesis over the pion hypothesis. We require that no energy be deposited in the back hadronic section of the LAC, and that between 3 and 25 electromagnetic LAC towers be hit in the associated cluster. In addition, if there are no unassociated neutral clusters within 10^o of the track, we require that the quasi-invariant mass be less than 500 MeV/c^2. If there are one or two unassociated clusters within

.

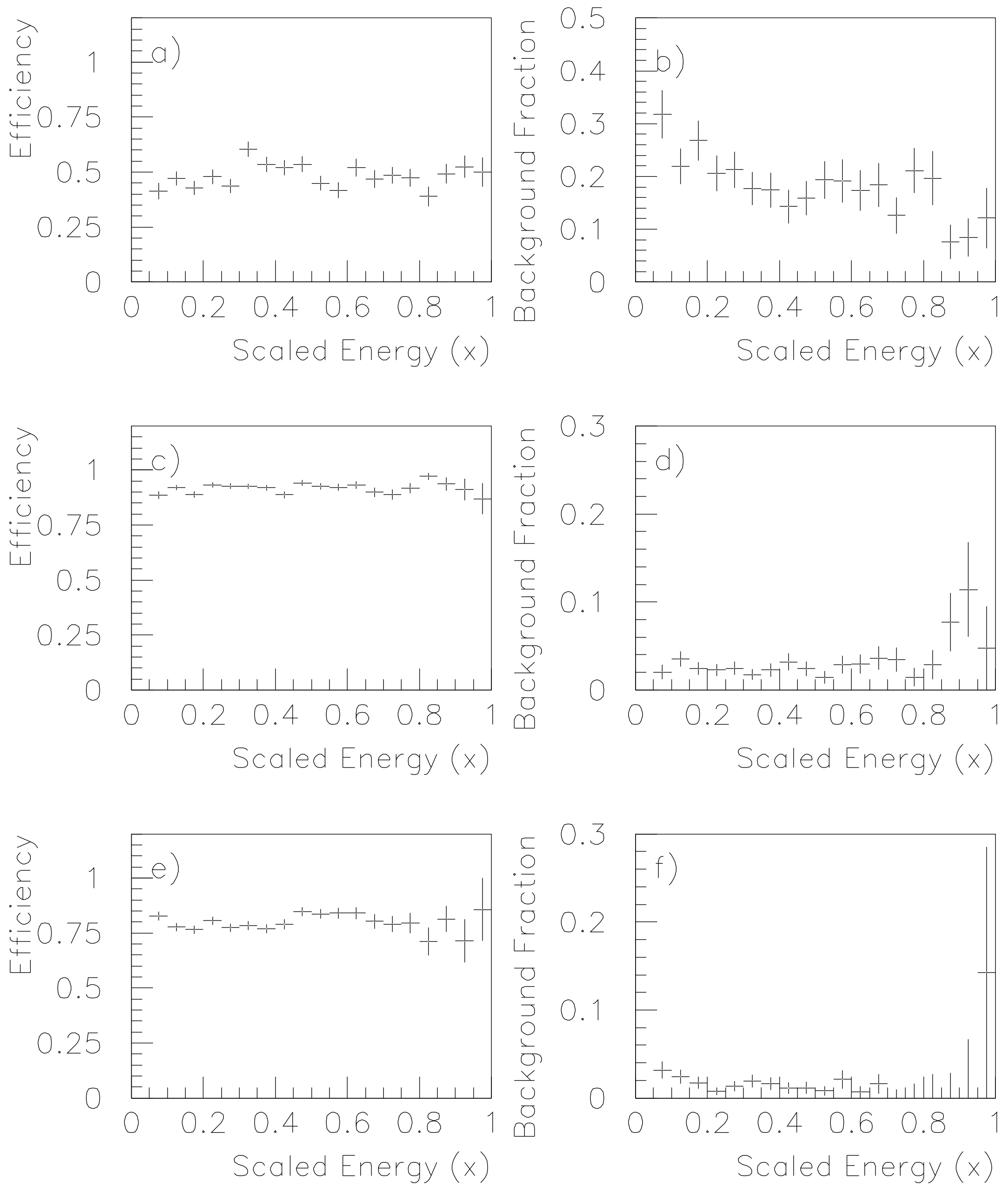

Figure 2: The MC estimated selection efficiency and background fractions versus scaled energy for tau decays to pions (a,b), muons (c,d), and electrons (e,f).

10^o of the track, we construct the invariant mass of the cone assuming the track is a pion and the clusters photons, and require this quantity to be less than 500 MeV/c^2. This results in a sample of 863 identified electron tracks with an estimated efficiency of 80% within the acceptance and an estimated purity of 98%. The efficiency and backgrounds versus scaled energy of these tracks are shown in Fig. 2(e) and 2(f).

4 Data Analysis

Section 1, and Fig. 1 in particular, show how the average polarization of the τ changes going from positive to negative electron beam polarization or from forward to backward scattering angles. Even before applying any corrections, one can clearly see in the SLD data the differences in the decay particle energy spectra due to different regions of P_e and $\cos\theta$. Fig. 3 shows the energy spectrum of $\tau\to\pi(\mathrm{K})\nu_\tau$ decays for both data and Monte Carlo, plotted separately for two regions of $(P_e, \cos\theta)$. Fig. 3(a) shows the spectrum for $P_e > 0$ and $\cos\theta < 0$ combined with $P_e < 0$ and $\cos\theta > 0$, while Fig. 3(b) is for events with $P_e > 0$ and $\cos\theta > 0$ together with events with $P_e < 0$ and $\cos\theta < 0$. The difference is expected to be less obvious in the three-body decays $\tau\to\ell\bar{\nu}_\ell\nu_\tau$, but is still quite visible as shown in Fig. 4.

The tau neutrino helicity, h_{ν_τ}, and the Michel parameters ξ and $\xi\delta$ are determined using an unbinned maximum likelihood fit to the energy spectra of the decay channels $\tau\to\pi(\mathrm{K})\nu_\tau$ and $\tau\to\ell\bar{\nu}_\ell\nu_\tau$. The fit function is the theoretical differential cross section (Eq. 8) corrected for radiative and detector effects.

In the maximum likelihood technique, the following expression is minimized:

$$W = -2\ln\mathcal{L} = -2\sum_{n=1}^{N}\ln\left\{\frac{1}{\sigma_i}\frac{d^2\sigma_i}{d\cos\theta\, dx_i}\right\}_n , \tag{10}$$

where $\mathcal{L}$ is the likelihood function. The sum in Eq. 10 runs over all τ's that have been identified as $\tau\to\mathrm{e}\bar{\nu}_e\nu_\tau$, $\tau\to\mu\bar{\nu}_\mu\nu_\tau$ or $\tau\to\pi(\mathrm{K})\nu_\tau$ candidates ($i = 1-3$ respectively). The term in the logarithm is the differential cross-section for production of τ-pairs where one τ decays into channel i. This expression is corrected for effects of radiation, detector resolution, efficiency and backgrounds, and is normalized to unity.

The corrected cross-section can be written in the following form,

$$\begin{aligned}\frac{16}{3}\frac{1}{\sigma_i}\frac{d^2\sigma_i}{d\cos\theta\, dx_i} &= \sum_{hel=\pm}\{\mathcal{E}_i^\pm(x_i,\cos\theta)\mathcal{U}^\pm(\cos\theta) \\ &\times\ [\epsilon_i(x_i,\cos\theta)\mathcal{V}_i^\pm(x_i) + \beta_i^\pm(x_i,\cos\theta)]\} \\ &+\ \beta_i^{non-\tau}(x_i,\cos\theta).\end{aligned} \tag{11}$$

Here $\mathcal{E}_i^\pm(x_i,\cos\theta)$ is the efficiency for selecting a τ-pair event in which one tau decays via channel $i(=\mathrm{e}, \mu, \pi)$; $\epsilon_i(x_i,\cos\theta)$ is the efficiency to identify the decay channel i; $\beta_i^\pm(x_i,\cos\theta)$

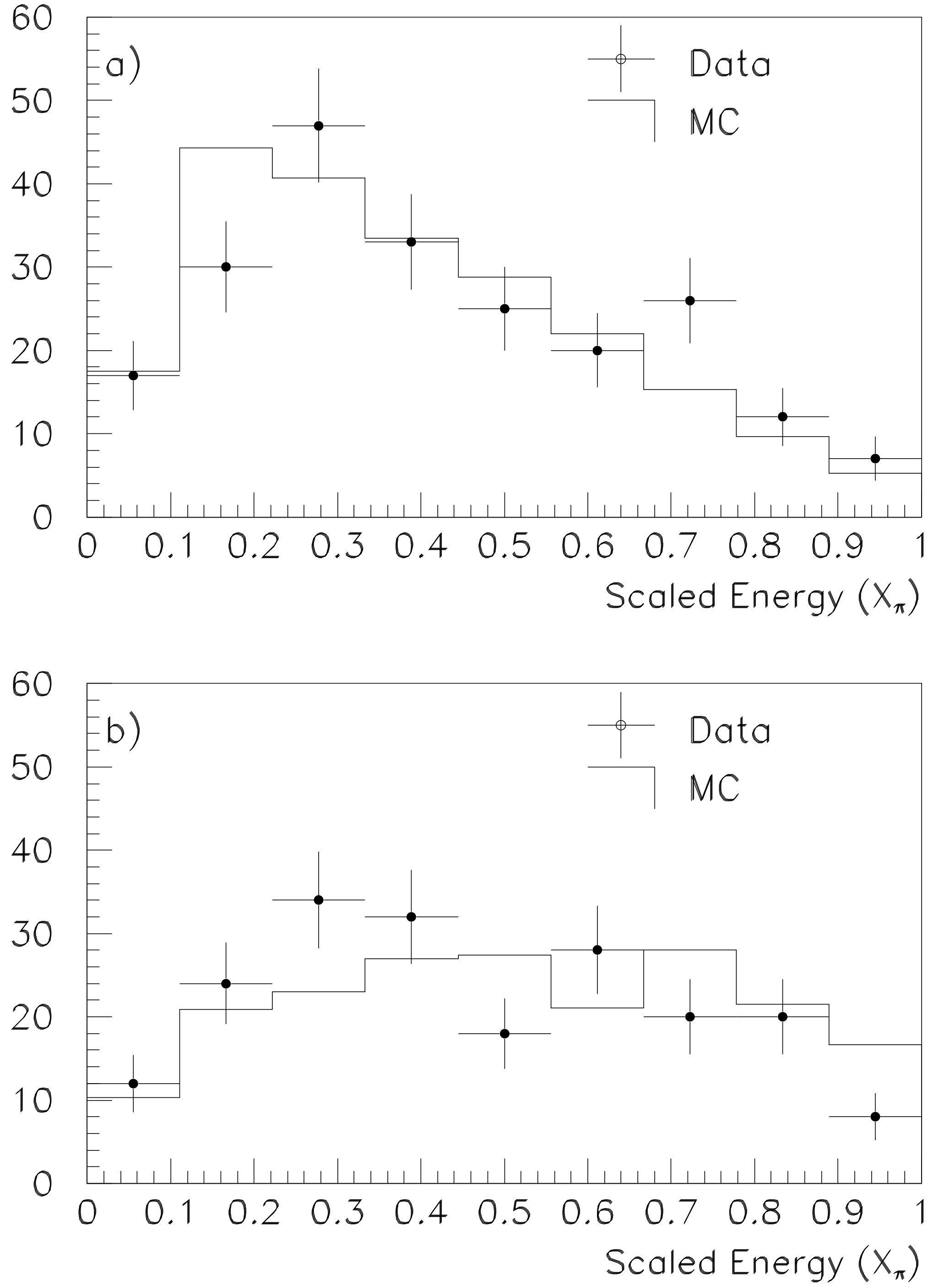

.

Figure 3: $\tau \to \pi(\mathrm{K})\nu_\tau$ decay energy spectra: (a) The sum of the spectra for pions in the forward direction with beam polarization $P_e < 0$ and in the backward direction with $P_e > 0$; (b) The sum of the spectra for pions in the backward direction with $P_e < 0$ and in the forward direction with $P_e > 0$. In each case the points are data and the histogram is from Monte Carlo.

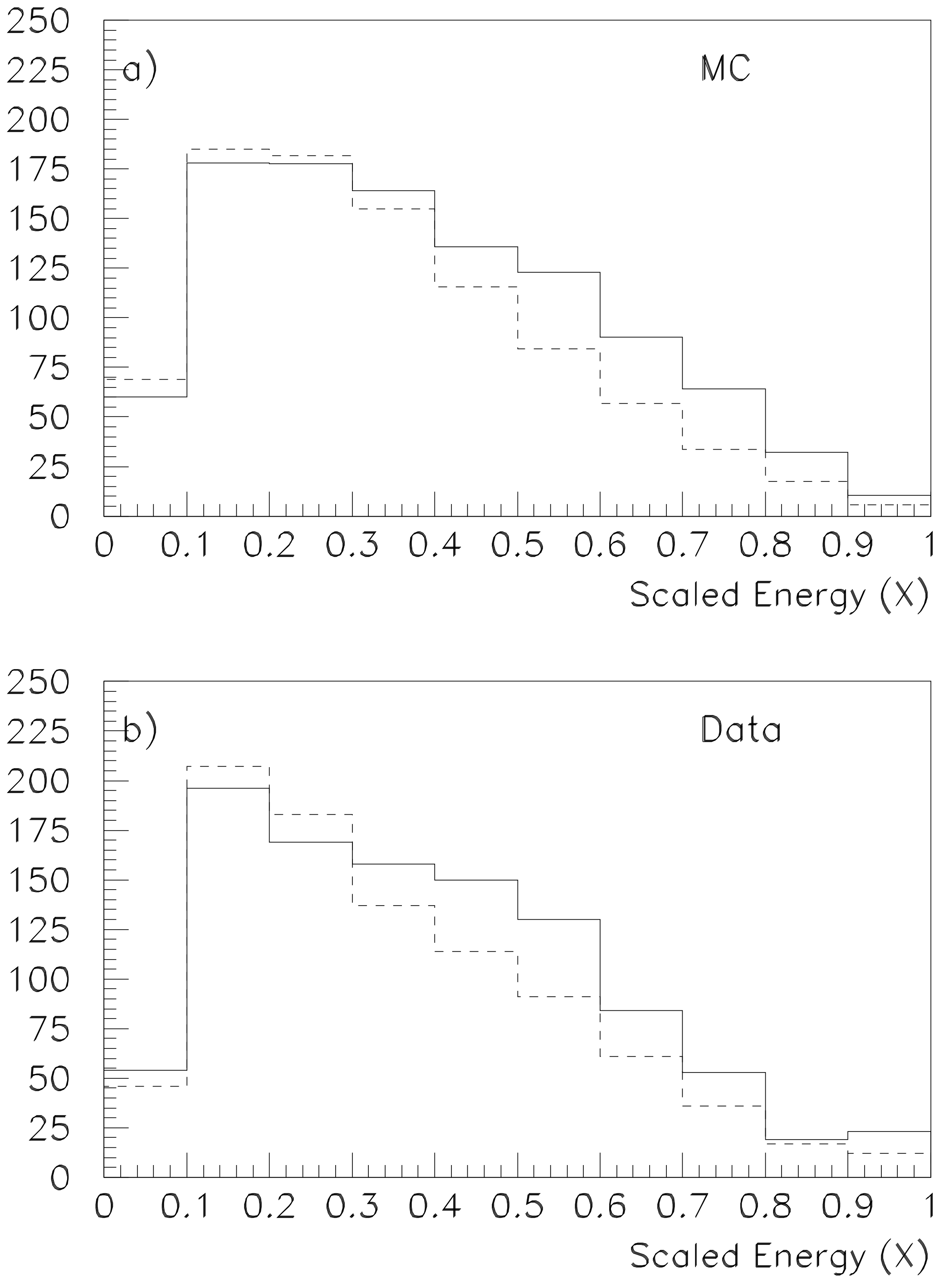

Figure 4: $\tau \rightarrow \ell \bar{\nu}_\ell \nu_\tau$ decay energy spectra from (a) Monte Carlo, and (b) the SLD data. For both histograms, the solid line is the sum of the spectra for leptons in the forward direction with beam polarization $P_e < 0$ and in the backward direction with $P_e > 0$, and the dashed line is the sum of the spectra for leptons in the backward direction with $P_e < 0$ and in the forward direction with $P_e > 0$.

corresponds to the distribution of contamination from misidentified τ decays; and $\beta_i^{non-\tau}(x_i, \cos\theta)$ is the background contribution from events which are not tau-pairs. These efficiencies and backgrounds were determined from Monte Carlo by studying the distribution of kinematic variables before and after event selection. The dependence of these functions on x and $\cos\theta$ were parameterized using low order polynomials.

The functions $\mathcal{V}_i^{\pm}(x_i)$ are obtained from the theoretical decay spectra $V_i^{\pm}(\bar{x}_i)$ after applying radiative corrections and convoluting with the detector resolution function:

$$\begin{aligned} \mathcal{V}_i^{\pm}(x_i) &= \int_0^1 V^{\pm}(\bar{x}_i) r_i^{\pm}(\bar{x}_i) \mathcal{R}_i(\bar{x}_i, x_i) d\bar{x}_i, \\ V_i^{\pm}(\bar{x}_i) &= f_i(\bar{x}_i) \pm g_i(\bar{x}_i). \end{aligned} \tag{12}$$

The functions $\mathcal{U}^{\pm}(\cos\theta)$ represent the differential cross-sections $U^{\pm}(\bar{x}_i)$ for production of τ-pairs with polarized electrons, corrected for detector resolution and radiative effects:

$$\begin{aligned} \mathcal{U}^{\pm}(\cos\theta) &= \int_{-1}^1 U^{\pm}(\cos\bar{\theta}) \hat{r}_i^{\pm}(\cos\bar{\theta}) \mathcal{C}_i(\cos\bar{\theta}, \cos\theta) d\cos\bar{\theta}, \\ U^{\pm}(\cos\bar{\theta}) &= (1 - P_e \mathrm{A}_e)(1 \pm \mathrm{A}_\tau)(1 + \cos\bar{\theta}^2) + 2(\mathrm{A}_e - P_e)(\mathrm{A}_\tau \pm 1)\cos\bar{\theta}. \end{aligned} \tag{13}$$

The $\mathcal{R}_i(\bar{x}_i, x_i)$, $\mathcal{C}_i(\cos\bar{\theta}, \cos\theta)$ represent the detector response functions, i.e. the distribution of the measured x_i, $\cos\theta$ for a given true $\bar{x}_i$, $\cos\bar{\theta}$, respectively. The radiative correction functions $r_i^{\pm}(\bar{x}_i)$ and $\hat{r}_i^{\pm}(\cos\bar{\theta})$ are determined from the ratio of the spectrum generated using KORALZ [11] for events containing radiative effects to the spectrum of events generated with the Born level cross-sections.

Eq. 6 shows that the statistical precision in the extraction of the ρ parameter is not enhanced by the beam polarization, and our systematic uncertainty in its measurement is relatively large. Since ρ is well measured elsewhere [16] [17], we have fixed its value to a world average. As δ appears in the expression only in the product $\xi\delta$, we fit for ξ and this product to reduce errors due to correlations.

5 Results and Discussion

Fitting the $\tau\to\pi(\mathrm{K})\nu_\tau$ sample yields $\mathrm{h}_{\nu_\tau} = -0.89 \pm 0.21(stat)$, which can be interpreted as twice the helicity of the tau neutrino. The fit to the $\tau\to\ell\bar{\nu}_\ell\nu_\tau$ channels gives $\xi = 1.17 \pm 0.35(stat)$ and $\xi\delta = 0.49 \pm 0.24(stat)$.

The sources of systematic error which have been considered in the analysis include τ-pair selection efficiency and background, decay identification efficiency and background, x and $\cos\theta$ resolution, uncertainties in the measurements of the beam energy and polarization, uncertainty in the value of A_ℓ [18], and the effect of fixing the ρ parameter. Table 1 summarizes the systematic errors in our analysis. To investigate these errors, each parameter used in the fitting program is modified in turn by its uncertainty, and the fit is redone to obtain new values of h_{ν_τ}, ξ and $\xi\delta$. The systematic errors assigned to the effect of fixing ρ are taken to be the differences from the fitted values of ξ and $\xi\delta$ when ρ is a free parameter. Any correlation between these input parameters is taken into account when combining the errors. Each error listed in Table 1 is a combination of several related contributions, and for the listed errors we assume they are not correlated. They are combined in quadrature to give the overall systematic error listed in the last row of the table.

	Δh_ν	$\Delta\xi$	$\Delta(\xi\delta)$
τ selection	0.01	0.03	0.05
Final-state selection	0.05	0.02	0.01
τ background	0.01	0.03	0.02
Non-τ background	0.01	0.03	0.04
Radiative corrections	0.02	0.10	0.02
$\cos\theta$ resolution	0.01	0.05	0.02
x resolution	0.01	0.07	0.06
Beam energy	0.02	0.04	0.05
Beam polarization	0.01	0.02	0.01
A_e, A_τ	0.01	0.03	0.02
ρ fixed		0.14	0.07
TOTAL	0.07	0.21	0.13

Table 1: Systematic uncertainties.

The large uncertainty assigned due to the fixed ρ parameter may be partly redundant with the systematic error introduced by the resolution in x. Both of these result from the preliminary parameterizations of this resolution for the lepton channels, but we have taken a conservative approach and quoted the errors separately. Another large contribution to the systematic uncertainty on ξ is the radiative correction, which affects the electron channel more strongly. The uncertainty in h_{ν_τ} is dominated by the π selection efficiency and the interference with the decay channels $\pi^\pm N\pi^0$ (ρ, a_1, etc...).

Including systematic errors, the SLD preliminary values for h_{ν_τ} and the Michel parameters ξ and $\xi\delta$ are

$$\begin{aligned} h_\nu &= -0.89 \pm 0.21(stat) \pm 0.07(syst), \\ \xi &= 1.17 \pm 0.35(stat) \pm 0.21(syst), \quad and \\ \xi\delta &= 0.49 \pm 0.24(stat) \pm 0.13(syst). \end{aligned}$$

The results are consistent with the Standard Model V-A predictions of -1, 1, $\frac{3}{4}$. These measurements provide an interesting cross check with other experimental results [16], [17],

[19] since this analysis does not rely on spin correlations and is the first measurement to be performed with polarized beams. These results demonstrate the power of polarized beams for probing deviations from the Standard Model in the weak couplings.

Acknowledgments

We thank the personnel of the SLAC accelerator department and the technical staffs of our collaborating institutions for their outstanding efforts on our behalf.

References

[1] Y.S. Tsai, *Phys. Rev.* **D4** (1971) 2821.

[2] L. Michel, *Proc. Phys. Soc.* **A63** (1950) 514.
C. Bouchiat and L. Michel, *Phys Rev.* **106** (1957) 170.

[3] K.Mursula, M. Roos, F. Scheck, *Nucl. Phys.* **B219** (1989) 321.
W. Fetscher H.J. Gerber, K.F. Johnson, *Phys Lett.* **B173** (1986) 102.

[4] SLD Design Report, SLAC-REPORT-273, May 1984.

[5] M.D. Hildreth *et al.,* "Performance of the SLD Central Drift Chamber", SLAC-PUB-6656 (1994), to appear in *IEEE Trans. on Nucl. Sci.*

[6] C.J.S. Damerell *et al.,* "Design and Performance of the SLD Vertex Detector, a 120 MPixel Tracking System", Proceedings of the 26th Int. Conf. on High Energy Physics, Dallas, Texas, August 1992;
M. Strauss *et al.,* "Performance of the SLD CCD Pixel Vertex Detector and Design of an Upgrade," Proceedings of the 27th Int. Conf. on High Energy Physics, Glasgow, Scotland, July 1994.

[7] D. Axen *et al.,* "The Lead Liquid Argon Sampling Calorimeter of the SLD Detector", *Nucl. Instr. Meth.* **A328**, 472 (1993).

[8] K. Abe *et al., Nucl. Inst. and Meth.* **A343** (1994) 74.

[9] A. C. Benvenuti *et al., Nucl. Inst. and Meth.* **A290** (1990) 353.

[10] SLD Collaboration, K. Abe *et al.,* "Measurement of the Tau Lifetime at SLD", *SLAC-PUB-95-6767*, April 1995, Submitted to *Phys. Rev. D.*

[11] S. Jadach, B.F.L Ward and Z. Was, *Comp. Phys. Comm.* **66** (1991) 276
S. Jadach, J.H. Kühn and Z. Was, *Comp. Phys. Comm.***64** (1991) 275.

[12] S. Jadach and B.F.L. Ward, "BHLUMI 3.11: $\mathcal{O}(\alpha)$ YFS Monte Carlo for Wide Angle Bhabha Scattering at SLC/LEP Energies", to be published.

[13] H. Aihara *et al., Phys. Rev. Lett.* **58**, 97 (1987), and references therein.

[14] T. Sjöstrand and M. Bengtsson, *Comp. Phys. Comm.* **43**, 367 (1987);
T. Sjöstrand, *Comp. Phys. Comm.* **39**, 347 (1986).

[15] GEANT program, version 3.21, CERN Application Software Group, *CERN Program Library* (1993). See R. Brun *et al.,* , GEANT3 User's Guide, CERN-DD/EE/84-1, CERN (1989).

[16] ARGUS collaboration, H. Albrecht *et al., Phys. Lett.* **B337** (1994) 383; *Phys.Lett.* **B349** (1995) 576.

[17] ALEPH Collaboration, D. Buskulic *et al., Phys. Lett.* **B346** (1995) 379.

[18] The LEP average asymmetries are $A_\tau = 0.1418 \pm 0.0075$, $A_\ell = 0.1464 \pm 0.0039$, LEP Electroweak Working Group, "A Combination of Preliminary LEP Electroweak Results for the 1995 Summer Conferences", LEPEWWG/95-02, August 1995;
The SLD asymmetry value is $A_e = 0.1551 \pm 0.0040$, M. Woods, "The SLD A_{LR} Result and Review of Weak Mixing Angle Results at SLC and LEP", Proceeding of the 1995 European Physical Society Meeting, Brussels, Belgium, July 1995;
The combined SLD and LEP asymmetry which we have used is $A_\ell = 0.15075 \pm 0.0028$.

[19] CLEO Collaboration, J. Bartelt *et al.,* "$\pi^-\pi^+$ Energy Correlation in τ Pair Events", Proceedings of the 27th Int. Conf. on High Energy Physics, Glasgow, Scotland, July 1994.